

## Photoinduced Energy Transfer in Poly(trimethylene terephthalate)

Wei-ang Luo,<sup>†</sup> Yujie Chen,<sup>‡</sup> Xudong Chen,<sup>\*,†</sup> Zhengfu Liao,<sup>§</sup> Kancheng Mai,<sup>†</sup> and Mingqiu Zhang<sup>\*,†</sup>

Key Laboratory for Polymer Composite and Functional Materials of the Ministry of Education, School of Chemistry and Chemical Engineering, Sun Yat-sen University, Guangzhou 510275, China, State Key Laboratory of Optoelectronic Materials and Technologies, School of Physics and Engineering, Sun Yat-sen University, Guangzhou 510275, China, and Faculty of Materials and Energy, Guangdong University of Technology, Guangzhou 510006, China

Received January 2, 2008; Revised Manuscript Received March 8, 2008

**ABSTRACT:** Photoinduced energy transfer in poly(trimethylene terephthalate) (PTT) was investigated by examining its excitation wavelength and concentration dependences of fluorescence in solutions. Accordingly, critical quench concentration and critical trap formation concentration were identified. Besides, studies of temperature effect on photoluminescence (PL) behavior of amorphous PTT film from  $-183$  to  $+177$  °C revealed that both fluorescence and phosphorescence emissions at low temperature can be attributed to monomers and traps. Phosphorescence quenching originated from the discontinuous increase of nonradiative processes. The corresponding quenching activation energies were estimated to be 13.5 kJ/mol for monomer phosphorescence quenching and 17.2 kJ/mol for exciplex phosphorescence quenching, respectively. Furthermore, the PL method proved to be able to monitor molecular relaxations (including  $\gamma$ -,  $\beta$ -, and  $\alpha$ -transitions) and cold crystallization in PTT film, which used to be measured by dynamic mechanical analysis (DMA) and differential scanning calorimetry (DSC), respectively.

## Introduction

Molecular configuration of poly(*m*-alkylene terephthalates) consists of rigid planar terephthaloyl groups alternating with a flexible methylene group sequence. Poly(trimethylene terephthalate) (PTT) is an odd-numbered polyester with  $m = 3$ , while poly(ethylene terephthalate) (PET) and poly(butylene terephthalate) (PBT) are even-numbered ones. Owing to the odd-carbon effect,<sup>1</sup> PTT fiber has high resilience and elastic recovery and can be used in carpet and other textile fiber applications.<sup>1–3</sup> In addition, PTT possesses superior processing properties with high physical, chemical, mechanical and thermal stability, which also has the most competitive predominance in the field of thermoplastic engineering plastics.<sup>4</sup> On the other hand, PTT has high birefringence and luminous transmittance, so that it is expected to be applied in the fields of optical communications, optical data processing, directional couplers and nonlinear optics.<sup>5,6</sup>

Numerous structural studies<sup>1,7–10</sup> have shown that structural differences are the main source of the discrepancy in physical properties between PET, PBT, and PTT. In crystalline phase, the conformations of *m*-methylene glycol segment are *trans-gauche-gauche-trans* (tggt) for PTT, *all-trans* for PET, and either *all-trans* or *gauche-gauche-trans-gauche-gauche* (gggtg) for PBT. The unit cell in PTT contains two monomer units forming a 2/1 helix, and the consecutive phenyl groups along the chain are inclined in opposite directions.

Because of extensively potential applications of PTT, it is imperative to gain deeper insight into its structure-properties relationship. So far, investigation of molecular motion and microstructures of polymers at molecular level by fluorescence techniques has attracted great attention. Photoluminescence (PL) method was employed for detecting real-time molecular motion

and microenvironment in polymers,<sup>11</sup> since it has merits of high sensitivity and nondestructive measurements. Yet, up to now, little work has been done on understanding intrinsic luminescence and relation between molecular chain motion and photophysical properties of PTT. This is particularly true for PTT films, mainly because the thicknesses and crystallinities of PTT films employed by different groups differed from one another.

Therefore, the goal of the present work is to clarify photoinduced energy transfer mechanism in PTT and to obtain in situ information about its structural relaxation. For this purpose, a detailed luminescence spectral analysis of PTT (in the forms of solution and film) is conducted. Molecular chain motion and evolution of microstructure are traced by studying temperature dependent PL of the polymer.

## Experimental Section

PTT, with an intrinsic viscosity of 0.91 dL/g (measured in 60/40 mixture of phenol/tetrachloroethane at 25 °C), was provided by Shell Chemicals Co. Prior to the experiments, PTT pellets were dried at 80 °C for 48 h under vacuum. PTT solutions with various concentrations were obtained by dissolving PTT pellets in chloroform–trifluoroacetic acid (4:1 v/v) mixed solvent. On the other hand, because PTT is a semicrystalline polymer, its amorphous film with a thickness of 20–30  $\mu$ m was obtained by melt-pressing at 260 °C for 5 min and subsequently quenching in ice–water.

PL emission spectra were collected with a combined fluorescence lifetime and steady state spectrometer (FLS920). The light source was a 450-W xenon lamp, while the spectral bandwidth was 1 nm for both excitation and emission monochromators. Experiments of PTT solutions were performed in a 1 cm path-length quartz cell at room temperature. Surface fluorescence was collected on a filter paper. Temperature-dependence measurements were carried out with the aid of a program-controlled closed-cycle liquid helium cryostat (ARS 8200), so that the temperature could be maintained with an accuracy of  $\pm 0.1$  °C during experiments. Polymer film (1 cm  $\times$  1 cm) was held in a copper frame. The available temperature ranged from  $-183$  to  $+177$  °C at a heating rate of 2 °C/min. In order to reduce reflection, the angle between excitation beam and the perpendicular to sample surface was chosen to be about 70°, and

\* Corresponding author. E-mail: cesxd@mail.sysu.edu.cn (X.C.); ceszmq@mail.sysu.edu.cn (M.Z.). Telephone and fax: +86-20-84113498.

<sup>†</sup> Key Laboratory for Polymer Composite and Functional Materials of the Ministry of Education, School of Chemistry and Chemical Engineering, Sun Yat-sen University.

<sup>‡</sup> State Key Laboratory of Optoelectronic Materials and Technologies, School of Physics and Engineering, Sun Yat-sen University.

<sup>§</sup> Faculty of Materials and Energy, Guangdong University of Technology.

fluorescence emission was collected at an angle of about 90° to the excitation beam.

The absorption spectra were recorded by a UV-vis-NIR spectrophotometer (UV-3150).

Differential scanning calorimetry (DSC) measurements were performed on a Perkin-Elmer DSC-7 under nitrogen conditions. The sample was heated from 0 to 100 °C at a heating rate of 10 °C/min. The instrument was calibrated with high purity melting standard indium and zinc.

## Results and Discussion

**1. PL Behavior of PTT Solutions.** Structural information of luminescence species could provide insight into interaction of molecular chains, like electron transfer and energy migration in the system.<sup>12</sup> According to the characteristics of segment density,<sup>13</sup> polymer solution can be classified into three categories: dilute, semidilute, and concentrated. For the transitions from dilute to semidilute to concentrated regimes, there exist two critical concentrations, denoted as  $C^*$  and  $C^+$ , respectively. Accordingly, the segment density undergoes a transit from discontinuous and nonuniform, continuous but still nonuniform, to continuous and uniform. A variety of methods have been proposed to measure the critical concentrations of the two transitions. For example, concentration and temperature dependences of polystyrene (PS) in hexane were measured by correlation spectroscopy, and the  $C^*$  value was determined by the minimum of the diffusion constant.<sup>14</sup> Daoud et al. studied radius of gyration as a function of concentration to find out  $C^*$ .<sup>15</sup> PL method has also been used to probe the solution transition.  $C^*$  and  $C^+$  were measured by investigating concentration dependence of PS excimer fluorescence.<sup>16</sup>

Here in this work, a study of PTT solutions in chloroform-trifluoroacetic acid (4:1 v/v) mixed solvent was performed, in order to select the appropriate excitation wavelength and to observe the chains in solution under different solution conditions. Figure 1 and Figure 2 show the emission spectra of PTT solutions excited by the light with different excitation wavelengths. For the dilute PTT solution ( $C = 0.1$  g/L), only monomer emission at 328 nm is observed (Figure 1, parts a and b). This is because neither interchain nor intrachain interactions are available due to the low segment intensity. The dependence of the 328 nm emission intensity on excitation wavelength is shown in Figure 1c. Clearly, the data go through a maximum at the wavelength of 305 nm. For concentrated PTT solution ( $C = 40$  g/L), a monomer emission is observed with excitation wavelength shorter than 320 nm (Figure 2). As displayed in Figure 2, the long wavelength tails of the emission become apparent with increasing excitation wavelength. The emission from 360 to 420 nm was assigned to the emission from traps, which was strongly influenced by polymer-solvent interactions,<sup>12</sup> but the details are not clear. To our knowledge, a solution most closely resembles the disordered nature of amorphous phase of a polymer solid. In fact, this new emission is well consistent with the surface fluorescence of PTT at about 390 nm (Figure 3). We have also recorded the excitation spectra for the fluorescence at 390 and 460 nm under the conditions that surface fluorescence was measured. It was found that the traps structure of PTT was excited by 315 nm light in solution, but this excitation wavelength was not such a good fit for 460 nm emission. However, 370 nm light was the best excitation wavelength for 460 nm emission, so the traps emission in the region of 360–420 nm may excite phosphorescence at about 460 nm due to reabsorption. In addition, the emission in the region 450 to 470 nm is due to phosphorescence, possibly from the monomeric unit.<sup>12</sup> Figure 2 also shows that a red shift (from 333 to 349 nm) in monomer emission maximum of PTT solution is accompanied by an increase in fluorescence intensity when excitation wavelength increases from 316 to 325 nm. This red-

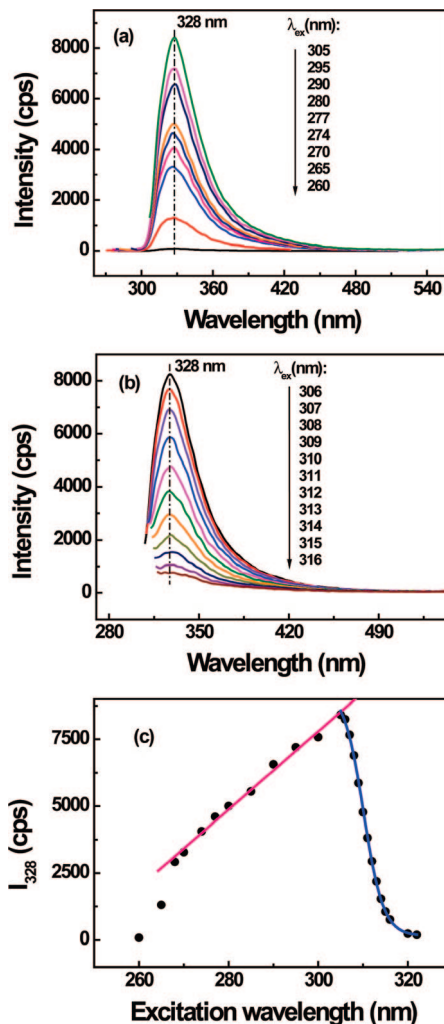


**Figure 1.** (a, b) Fluorescence spectra of PTT solution ( $C = 0.1$  g/L) with different excitation wavelengths and (c) PL intensity at 328 nm as a function of excitation wavelength.

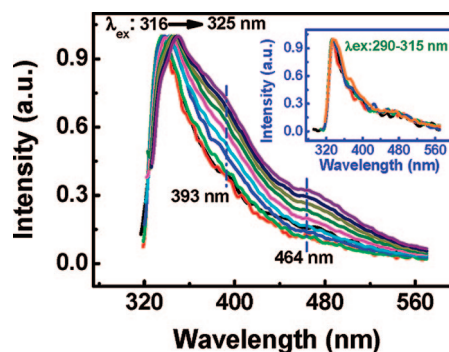


**Figure 2.** Fluorescence spectra of PTT solution ( $C = 40$  g/L) with different excitation wavelengths. The inset gives the normalized curves.

shift in wavelength of the maximum fluorescence emission, caused by a shift in excitation wavelength toward the red edge of the absorption band, is known as the “red-edge” effect (REE). It is mostly observed with polar fluorophores in motionally restricted media such as very viscous solutions or condensed phases. It is based on differential extents of solvent reorientation around the excited-state fluorophore, with each excitation wavelength selectively exciting a different average population of fluorophores.<sup>17</sup> These phenomena can be explained by the fact that segment-segment interaction becomes available in such

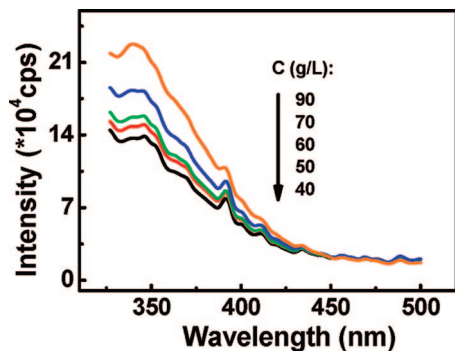


**Figure 3.** Surface fluorescence of PTT concentrated solutions ( $\lambda_{\text{ex}} = 315$  nm).

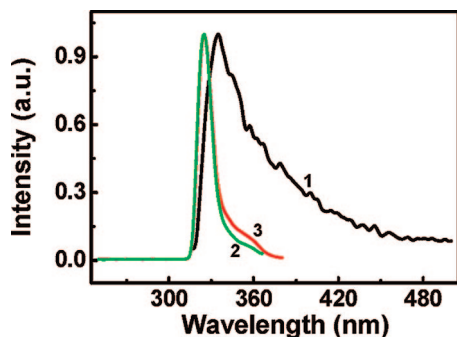


**Figure 4.** Excitation and emission spectra of PTT solution ( $C = 40$  g/L). Curve 1: Emission spectrum, excited at 315 nm. Curves 2 and 3: Excitation spectra, emission at 390 and 376 nm, respectively.

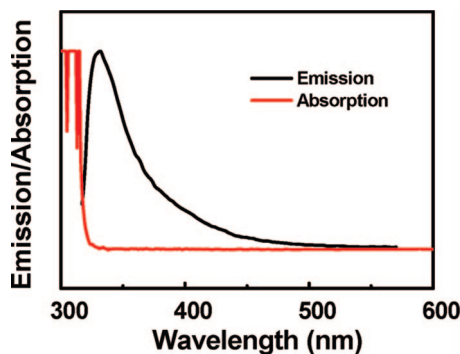


**Figure 5.** Absorption and emission spectra of PTT solution ( $C = 8$  g/L).

a concentrated solution. Consequently, energy transfer from monomer to traps (ground-state dimer, excimer, and/or exciplex) would happen,<sup>12</sup> resulting in a red-shift of maximum fluorescence emission and an increase of traps fluorescence intensity. Figure 4 shows the monomer emission spectrum (excitation at 315 nm) and excitation spectra of PTT trap (emission at 376 and 390 nm) in solution. The obvious overlap between emission and excitation spectra is indicative of the possibility that the fluorescing structure of trap might absorb the monomer emission at 329 nm before being excited. In previous reports, appearance of a red-shifted excitation spectrum was attributed to the presence of a ground-state dimer formed between adjacent aromatic side groups in poly(vinylnaphthalene).<sup>18</sup> Similar results were perceived in PET solution.<sup>19</sup> Furthermore, as shown in Figure 5, the emission and absorption spectra overlap each other when the concentration of PTT solution is higher than 8 g/L. High-energy photons (monomer fluorescence) are more likely reabsorbed, such that multiple reabsorption-reemission events cause a well-known red-shift in the observed fluorescence spectra and an increase in the trap fluorescence.<sup>20</sup>

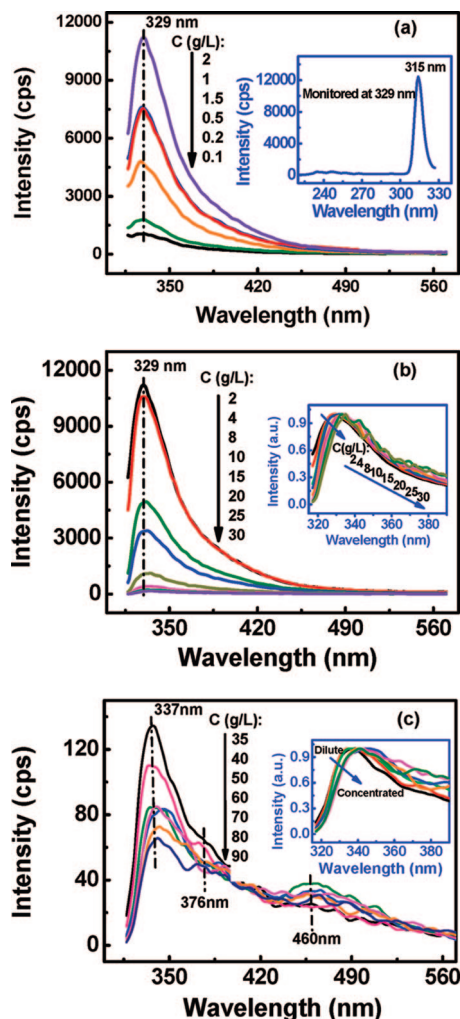


**Figure 6.** Concentration dependence of fluorescence spectra of PTT solution ( $\lambda_{\text{ex}} = 315$  nm). The inset in part a is the excitation spectrum of PTT solution of a concentration of 2 g/L ( $\lambda_{\text{em}} = 329$  nm). The insets in parts b and c show the normalized versions of the curves in parts b and c, respectively.

From the above analysis, it is known that monomer fluorescence is excited in dilute PTT solution, and in concentrated solution, the fluorescence is dependent on concentration, excitation wavelength, and solvent polarity.

To gain an in-depth understanding of the energy migration from monomer units to traps and structural characteristics of traps as well, concentration dependence of PTT luminescence was studied. In consideration of the excitation wavelength dependence of PTT solution fluorescence, the maximum monomeric excitation wavelength (315 nm) of a semidilute solution (2 g/L) was selected (see the inset in Figure 6a). Figure 6 presents PL spectra of PTT solutions with different concentrations excited by 315 nm. Obviously, two critical concentrations are perceived. That is, (i) critical quench concentration of 2 g/L (denoted as  $C_Q$ ), and (ii) critical traps formation concentration of 35 g/L (denoted as  $C_T$ ). As exhibited in Figure 3, parts a and b, the monomer fluorescence at 328 nm increases initially with a rise in solution concentration, reaching a maximum at the concentration of 2 g/L, and then quenches. Moreover, when the solution concentration is lower than 35 g/L, only monomer fluorescence peaks appear. Traps emission can be detected only when the concentration exceeds 35 g/L (Figure 6c). These phenomena may be explained by the fact that when solution concentration is lower than  $C_Q$ , the fluorescence intensity will increase with increasing the concentration because of the



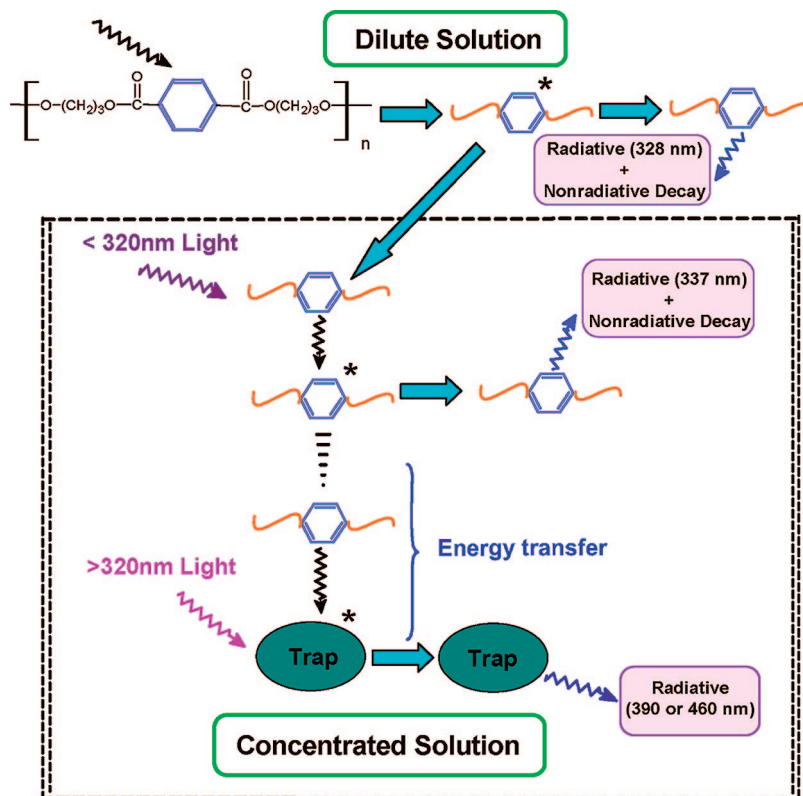


Figure 7. Luminescence model of PTT solution.

increase of the chromophores (Figure 6a).<sup>21</sup> When the concentration is higher than  $C_Q$  but lower than  $C_T$ , molecules in the system become more concentrative, and the emission intensity has to decrease (Figure 6b) and maximum fluorescence emission shifts to long wavelength region (see inset in Figure 6b) due to reabsorption.<sup>12</sup> However, in the case of sufficiently high concentration ( $> C_T$ ), segment density is significantly enhanced as a result of coiling and overlapping of PTT chains. Because of reabsorption, monomer unit could migrate energy to trap, it emits at the region of 360–420 nm as soon as the trap is excited, thus interchain or intrachain interactions among the phenylene moieties and/or among phenylene and carbonyl groups would lead to formation of dimer, excimer and/or exciplex.<sup>12,13</sup> Besides, reabsorption of the monomer unit itself will radiate lower energy<sup>20</sup> and produce an phosphorescence emission at about 460 nm. Red-shift effect also appears in these concentrated solutions (see the inset in Figure 6c).

To summarize the discussion of Figure 2 and 6, the photo-induced energy transfer of PTT excitons in solution can be expressed by the model schematically presented in Figure 7. In dilute solution, only monomer radiates at 329 nm. On the other hand, in semidilute and concentrated solutions, there exist two situations: (i) excited with a light shorter than 320 nm, monomer radiation shifts to longer wavelength region, and (ii) excited with a light longer than 320 nm, new emission appears at about 390 and 460 nm due to reabsorption.

Figure 8 displays the concentration dependence of monomer emission of PTT at different excitation wavelengths ( $\lambda_{ex} \leq 320$  nm). What is interesting is that the critical quench concentration increases with a rise in excitation wavelength. As shown in the inset of Figure 8, the denary logarithm of  $C_Q$  increases monotonically with increasing excitation wavelength. These phenomena should be a consequence of the coordinated action between excitation energy and segment density. Fewer monomers are excited due to the decrease in excitation energy as the excitation wavelength increases, reducing the probability of

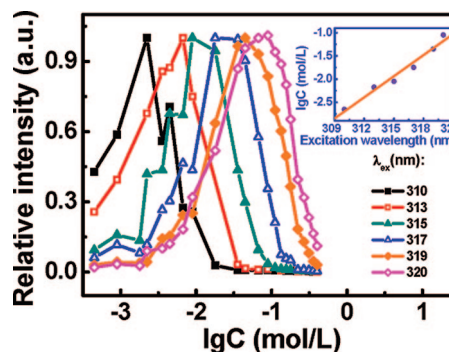
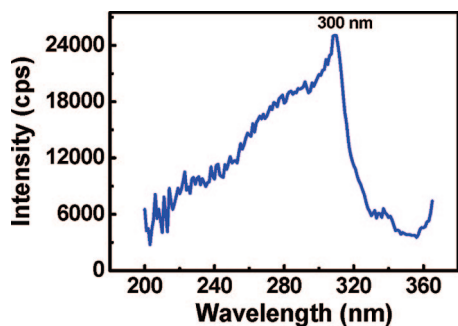


Figure 8. Concentration dependence of monomer emission of PTT solutions at different excitation wavelengths (values in each series are normalized to the solution of the highest fluorescence intensity).

collision between the excited monomers. However, in a relatively concentrated solution ( $< C_T$ ), a decreased radius of gyration due to polymer self-avoidance, would promote intra-chain contacts and monomer collision. That is to say, the decrease of excitation and increase of solution concentration will both accelerate the quench of monomers. Therefore, the critical quench concentration increases with increasing excitation wavelength. Similar results were reported in the investigation of PET in 1, 1, 1, 3, 3, 3-hexafluoroisopropanol. It was found that owing to the chain coil in semidilute solution, monomer excitation spectra shifted toward longer wavelength with increasing solution concentration.<sup>13</sup>

**2. Temperature Dependent Photoluminescence of PTT Film.** In the last subsection, the photoinduced energy transfer mechanism in PTT has been clarified. On the basis of this outcome, the dynamic process of molecular motion of PTT can be inspected by investigating the temperature dependence of photoluminescence of an amorphous PTT film. It will reveal the information about structural relaxations in the polymer.



**Figure 9.** Excitation spectrum of PTT film at room temperature ( $\lambda_{\text{em}} = 374$  nm).

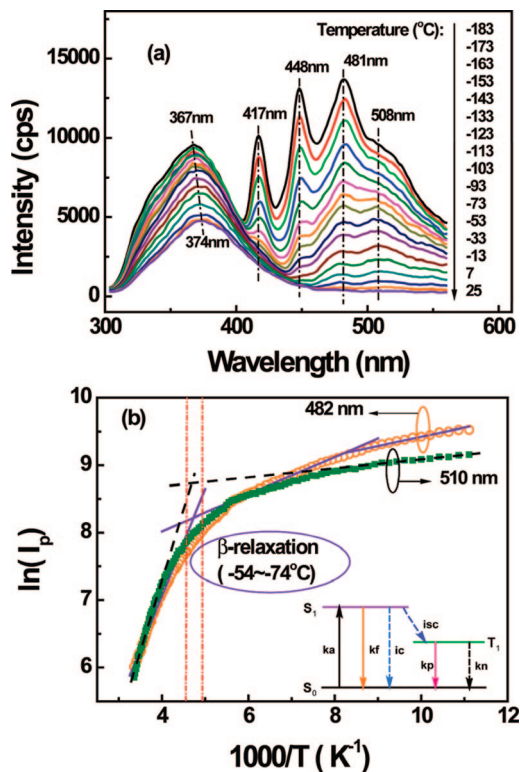


**Figure 10.** (a) Temperature-dependent PL spectra of amorphous PTT film ( $\lambda_{\text{ex}} = 300$  nm), and (b) Arrhenius curves for PTT phosphorescence. The inset in (b) is the simplified Jablonski diagram.  $k_a$ ,  $k_f$ , and  $k_p$  are the rate constants for absorption, fluorescence, and phosphorescence, respectively.  $k_n$  is the rate sum of all the other nonradiative processes from the triplet state.  $i_{\text{sc}}$  is the intersystem crossing, and  $i_c$  is the internal conversion.

As shown in Figure 9, the amorphous PTT film exhibits a maximum excitation at 300 nm. Therefore, all the PL experiments of the PTT film were excited at 300 nm.

Figure 10a shows the temperature-dependent PL spectra of the amorphous PTT film from  $-183$  to  $+25$  °C at an excitation wavelength of 300 nm. The results are summarized as follows. (i) Compared with the fluorescence spectra of PTT solutions, the monomer fluorescence at around 330 nm is not obvious. (ii) The fluorescence peak near 370 nm is red-shifted from 367 to 374 nm with increasing temperature. (iii) At low temperature, structured phosphorescence emission peaks appear at 417, 448, 481, and 508 nm, respectively.

According to the PL behavior of PTT solutions and previous reports about PET film, it is known that the fluorescence of amorphous PTT film below 25 °C results from neither dimer nor excimer. Since the traps (dimer, excimer, or exciplex) emission emerges only in concentrated solution and could be

excited by light with its wavelength longer than 320 nm, we can rule out the possibility of ground-state dimer. Moreover, this fluorescence is quite different from the reported emission of PET dimer (absorption peak at 340 nm and fluorescence peak at 390 nm).<sup>12,22</sup> In fact, the possibility of excimer fluorescence can also be excluded because the peak of an excimer emission should be constant. In this context, the red-shift phenomenon in fluorescence should be attributed to the interaction among phenylene groups and/or phenylene and carbonyl groups, which plays an important role in stabilization of the excited monomer state of phenylene moiety.<sup>23,24</sup>

With respect to the structured phosphorescence emissions at 417, 448, 481 and 508 nm at low temperature, the peaks in the region of 410–485 nm correspond to monomeric phosphorescence of  $^3(\pi-\pi^*)$  states, and that at around 510 nm would be associated to the exciplex due to the interaction between excited C=O and phenyl ring. Previous report indicated that the phosphorescence emission at 480 nm originated from monomeric unit of polymers.<sup>19</sup> These results coincide with those of PET reported by Teyss  re et al.<sup>21</sup> It is noted that the temperature-dependent PL spectra of PET show fluorescence emission at 368 nm, which does not shift to long wavelength as the fluorescence of PTT film. Moreover, PET film has phosphorescence at 540 nm, but PTT film has not. The fluorescence at 368 nm and the phosphorescence in the range 480–540 nm were believed to be the result of a ground-state dimer.<sup>21</sup> The difference in luminescence between PET and PTT should originate from the difference in their microstructures.

As shown in Figure 10a, the phosphorescence decreases as temperature is raised. From the simplified Jablonski diagram (see the inset of Figure 10b), it is obvious that the decrease in phosphorescence can be attributed to the discontinuous increase of some nonradiative process included in the  $k_n$  term.<sup>25</sup> The  $k_n$  presumably follows the Arrhenius relationship:  $I_p \sim k_n \exp(-E/RT)$ , where  $E$  is the activation energy for the phosphorescence quenching,  $R$  is the gas constant, and  $I_p$  is the phosphorescence intensity. Because the lifetime of triplet-excited states in phosphorescence is longer than that of singlet-excited states in fluorescence, it is easy for them to transfer their energy to the surroundings, thus quenching the emission. Figure 10b gives the Arrhenius curve of  $\ln(I_p)$  vs  $1/T$ . Accordingly, the activation energy for monomer phosphorescence quenching is estimated to be 13.5 kJ/mol and that for exciplex phosphorescence quenching 17.2 kJ/mol.

For amorphous polymers, molecular relaxations are always related to their chemical structures and dynamics of the molecular chains. In general, small-scale motions of backbone or side-chain segments with low activation energies account for the relaxation processes. Considering that temperature dependence of phosphorescence is also associated with local molecular motion,<sup>21</sup> mechanical relaxation and phosphorescence can thus be correlated on the basis of their temperature dependences.

Figure 10a shows that the short wavelength part of the phosphorescence spectra (417 nm) disappears when temperature is higher than  $-103$  °C, then the emission at around 448 nm disappears at  $-63$  °C, whereas the longer wavelength part is still detectable at room temperature. It is interesting to see that the temperatures at which the two short wavelength phosphorescence emissions disappear are right consistent with the temperatures of  $\gamma$ -transition ( $-118$  °C) and  $\beta$ -transition ( $-66$  °C) of PTT film measured by dynamic mechanical analysis (DMA).<sup>26</sup> Early studies indicated that  $\beta$ -relaxation is produced by joint movements of phenyl, carboxyl, and  $\text{CH}_2$  sequence,<sup>26–30</sup> and  $\gamma$ -relaxation originates from movements of  $\text{CH}_2$  sequence containing at least three consecutive methylene units.<sup>26</sup> The transition temperatures could be influenced by crystallinity, cross-linking, structure of the repeating unit, and/or the presence

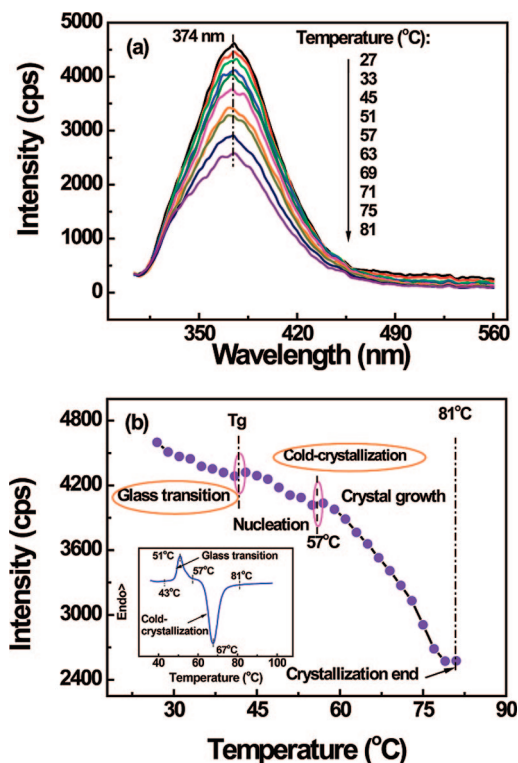


**Figure 11.** (a) Temperature-dependent PL spectra of amorphous PTT film, and (b) PL intensity as a function of temperature ( $\lambda_{\text{ex}} = 300$  nm). The inset in part b shows the DSC heating trace of the amorphous PTT film.

of diluents or plasticizers.<sup>25</sup> Since temperature dependence of phosphorescence proves to be able to reflect structural relaxations in PTT, the microstructural knowledge obtained by conventional DMA should in turn be used to interpret the optical performance of PTT film.

In the temperature range 27–81 °C, only a single emission peak is observed at 374 nm (Figure 11a). The peak intensity decreases with increasing temperature. It is due to a gradual transition of the main chain phenylene rings in amorphous form to crystalline. Figure 11b plots the temperature-dependent PL intensity at 374 nm. Two break-points appear on the curve at 41 and 57 °C, respectively. In fact,  $\alpha$ -transition of PTT film (i.e., glass transition), which involves motions of long segments, occurs at 43–57 °C. When temperature is higher than 57 °C, cold crystallization takes place up to 81 °C (see the inset in Figure 11b). The results demonstrate that both glass transition and cold crystallization of amorphous PTT film reflected by DSC can be exactly detected by fluorescence.

A crystallographic study of PTT suggested that the interplanar spacing of the two nearest phenylene rings is 0.554 nm.<sup>2</sup> It means that the  $\pi$ -electrons of the phenylene groups are isolated from each other. This explains why the phenylene fluorescence in crystalline region is identical to that in solution and excimer formation is impossible in the crystalline region. On the contrary, some phenylene moieties in the amorphous region can be within a distance of 0.35 nm from a phenylene or carbonyl group; thus, the  $\pi$ -electrons of phenylene groups might overlap and interact with the  $\pi$ -electrons of other phenylene groups and/or carbonyl groups.<sup>24</sup> In this context, the fluorescence of 374 nm must be the emission coming from the phenylene groups in the amorphous region of PTT film, with its intensity dependent on crystallinity. This finding could be applied to monitor dynamic change in cold-crystallization of the PTT solid.

Figure 12 shows the temperature-dependent PL spectra of the PTT film at temperatures higher than 81 °C. Two fluores-

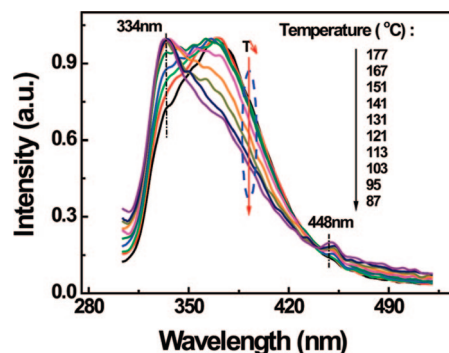


**Figure 12.** Effect of temperature on fluorescence spectra of the amorphous PTT film ( $\lambda_{\text{ex}} = 300$  nm, and each curve is normalized to the highest fluorescence intensity).

cence peaks appear at around 334 and 448 nm, which represent fluorescence and phosphorescence emissions of the PTT monomer, respectively. With a rise in temperature, the intensity of the peak at 334 nm gradually decreases, while that at 448 nm increases. This testifies to the fact that the emissions at 334 and 448 nm should be attributed to the same luminescent species. Itagaki and Kato considered that the 334 nm fluorescence resulted from the main-chain phenylene groups in crystalline region.<sup>31</sup> Accordingly, the peak at 448 nm must also be related to this segmental unit. It is worth noting that the fluorescence peak at 369 nm, which corresponds to the excimer luminescence, increases with increasing temperature. The enhancement of the excimer fluorescence keeps in step with the reduction in the monomer luminescence.<sup>23</sup> These phenomena further manifest that the PL spectra are capable of showing the gradual increase in crystallinity of amorphous PTT film with increasing temperature, the general law of semicrystalline polymers.

PL behaviors of PET and PBT have been well reported. The peaks at around 330 and 370 nm, which correspond to the crystalline and amorphous regions, respectively, were believed to be indicative of the microenvironment of main-chain phenylene.<sup>23,24,31,32</sup> Nevertheless, it is worth noting that the microenvironment dependence of phenylene is different in PET,<sup>24</sup> PBT,<sup>23</sup> and PTT. Itagaki et al.<sup>24,31,32</sup> studied the PL of PET films cast on quartz disks. They found that the fluorescence peak shifted from 355 to 360 nm when cast temperature changed from 40 to 160 °C. They also investigated the microenvironment in spin-casting PBT films via PL method.<sup>23</sup> The results indicated that there were two fluorescence peaks at 325 and 365 nm, reflecting monomer fluorescence in the crystalline region and excimer fluorescence in the amorphous phase, respectively. Both the peak positions were constant with a rise in cast temperature (from 60 to 200 °C). However, in our real-time investigation on PL behavior of the melt-quench PTT film, only a single fluorescence emission assigned to excimer was perceived at 374 nm within temperature range between 27 and 81 °C. When the temperature exceeded 81 °C, monomer emission at 334 nm and excimer emission at 369 nm emerged.

In addition, the position of fluorescence peak of polyester's monomer or excimer exhibits an odd–even effect. The odd-numbered polyester, PTT, has the longest wavelength fluorescence emission. Similar conclusions were made by Mendicuti et al.,<sup>33</sup> who attributed the red-shift of the emission band to formation of the excimer. By using rotational isomeric state analysis, they identified the conformations conducive to excimer formation and calculated the dependence of probabilities of excimer formation on methylene number. The result implied that PTT had the highest probability to form excimer as compared with PBT and PET. The methylene segments in PTT are long enough to isolate each  $\pi$ -electrons of terephthalate



moieties. When the temperature is higher than the glass transition temperature, terephthalate moieties can be settled down in the stable configuration forming excimer.<sup>23</sup> In addition, for PTT, the terephthaloyl residues are more mobile than CH<sub>2</sub> groups, but for PBT, the central CH<sub>2</sub> groups become the most mobile.<sup>34</sup> These would also induce different PL behaviors in PTT and PBT.

### Conclusions

The dependences of PL behavior of PTT solution on excitation wavelength, solution concentration and temperature were investigated. The dilute solution and the concentrated solution exhibited different dependences on excitation wavelength. Accordingly, two critical concentrations were identified. A reasonable interpretation for the photoinduced energy transfer mechanism in PTT lies in that the self-absorption led to the concentration quench effect, and the combined interaction of excitation energy and segment density resulted in the formation of traps.

Detailed investigation on the molecular mobility and evolution of emission species during the gradual heating of amorphous PTT films was performed. The relaxations and cold-crystallization reflected by PL method are in good agreement with those measured by DMA and DSC studies, respectively. Therefore, a new characterization technique for revealing molecular movements in terms of PL spectra might thus be developed on the basis of this finding.

The difference in fluorescence properties of PET, PBT, and PTT was considered to be due to their different microconformations of molecular chains. The longer-wavelength fluorescence at about 370 nm demonstrated an odd–even effect.

**Acknowledgment.** X.C. acknowledges financial support from the program of National Natural Science Foundation of China (Grant No. 50673104) and Natural Science Foundation of Guangdong Province (Grant No. 7003702).

### References and Notes

- (1) Kim, K. J.; Bae, J. H.; Kim, Y. H. *Polymer* **2001**, *42*, 1023.
- (2) Wu, G.; Li, H. W.; Wu, Y. Q.; Cuculo, J. A. *Polymer* **2002**, *43*, 4915.

- (3) Chang, J.-H.; Kim, S. J.; Im, S. *Polymer* **2004**, *45*, 5171.
- (4) Brown, H. S.; Chuah, H. H. *Chem. Fibers Int.* **1997**, *47*, 72.
- (5) Singh, G. K.; Low, A. L. Y.; Yong, Y. S. *Optik* **2004**, *115* (7), 334.
- (6) Bai, S. J.; Spry, R. J.; Alexander, M. D., Jr.; Barkley, J. R. *J. Appl. Phys.* **1996**, *79* (12), 9326.
- (7) Pellerin, C.; Pézolet, M.; Griffiths, P. R. *Macromolecules* **2006**, *39*, 6546.
- (8) Chuah, H. H. J. *Polym. Sci., Part B: Polym. Phys.* **2002**, *40*, 1513.
- (9) Jeong, Y. G.; Bae, W. J.; Jo, W. H. *Polymer* **2005**, *46*, 8297.
- (10) Frisk, S.; Ikeda, R. M.; Chase, D. B.; Kennedy, A.; Rabolt, J. F. *Macromolecules* **2004**, *37*, 6027.
- (11) Itagaki, H.; Horie, K.; Mita, I. *Prog. Polym. Sci.* **1990**, *15*, 361.
- (12) Hemker, D. J.; Frank, C. W. *Polymer* **1988**, *29*, 437.
- (13) Sonnenschein, M. F.; Roland, C. M. *J. Polym. Sci., Part B: Polym. Phys.* **1991**, *29*, 431.
- (14) Munch, J. P.; Ankrim, M.; Hild, G.; Okasha, R.; Candau, S. *Macromolecules* **1984**, *17*, 110.
- (15) Daoud, M.; Cotton, J. P.; Farnoux, B.; Jannink, G.; Sarma, G.; Benoit, H.; Duplessix, R.; Picot, C.; Gennes, P. G. D. *Macromolecules* **1975**, *8*, 804.
- (16) Qian, R. Y.; Gu, X. H. *Angew. Makromol. Chem.* **1986**, *141*, 1.
- (17) Chattopadhyay, A.; Mukherjee, S.; Raghuraman, H. *J. Phys. Chem. B* **2002**, *106*, 13002.
- (18) Irie, M.; KamiJo, T.; Aikawa, M.; Takemura, T.; Hayashi, K.; Baba, H. *J. Phys. Chem.* **1977**, *81*, 1571.
- (19) Allen, N. S.; McKellar, J. F. *Macromol. Chem.* **1978**, *179*, 523.
- (20) Hidrovo, C. H.; Hart, D. P. *Meas. Sci. Technol.* **2001**, *12*, 467.
- (21) Teyssèdre, G.; Menegotto, J.; Laurent, C. *Polymer* **2001**, *42*, 8207.
- (22) Hennecke, M.; Fuhrman, K. K. J. *Colloid Polym. Sci.* **1987**, *265*, 674.
- (23) Itagaki, H.; Arakawa, S. *Polymer* **2003**, *44*, 3921.
- (24) Itagaki, H.; Inagaki, Y.; Kobayashi, N. *Polymer* **1996**, *37*, 3553.
- (25) Somersall, A. C.; Dan, E.; Guillet, J. E. *Macromolecules* **1974**, *7*, 233.
- (26) Gonzalez, C. C.; Perena, J. M.; Bello, A. J. *Polym. Sci., Part B: Polym. Phys. Ed.* **1988**, *26*, 1397.
- (27) Kalakkunnath, S.; Kalika, D. S. *Polymer* **2006**, *47*, 7085.
- (28) Mackintosh, A. R.; Liggat, J. J. *J. Appl. Polym. Sci.* **2004**, *92*, 2791.
- (29) Maxwell, A. S.; Monnerie, L.; Ward, I. M. *Polymer* **1998**, *39*, 6851.
- (30) Corrales, T.; Peinado, C.; Bosch, P.; Catalina, F. *Polymer* **2004**, *45*, 1545.
- (31) Itagaki, H.; Kato, S. *Polymer* **1999**, *40*, 3501.
- (32) Itagaki, H. *J. Lumin.* **1997**, *435*, 72.
- (33) Mendicuti, F.; Patel, B.; Viswanadhan, V. N.; Mattice, W. L. *Polymer* **1988**, *29*, 1669.
- (34) Horii, F.; Hirai, A.; Murayama, K.; Kitamaru, R.; Suzuki, T. *Macromolecules* **1983**, *16*, 273.

MA8000059